



## RESEARCH ARTICLE

# Clinical relevance of molecular subgrouping of gliomatosis cerebri per 2016 WHO classification: a clinicopathological study of 89 cases

Mi Jung Kwon<sup>1</sup> ; SoYoung Kang<sup>2</sup>; Haeyon Cho<sup>2</sup>; Jung Il Lee<sup>3</sup>; SungTae Kim<sup>4</sup>; Yeon-Lim Suh<sup>2</sup> 

<sup>1</sup> Department of Pathology, Hallym University Sacred Heart Hospital, Hallym University College of Medicine, Anyang, South Korea.

<sup>2</sup> Department of Pathology, Samsung Medical Center, Sungkyunkwan University College of Medicine, Seoul, South Korea.

<sup>3</sup> Department of Neurosurgery, Samsung Medical Center, Sungkyunkwan University College of Medicine, Seoul, South Korea.

<sup>4</sup> Department of Radiology, Samsung Medical Center, Sungkyunkwan University College of Medicine, Seoul, South Korea.

## Keywords

disease progression, gliomatosis cerebri, histology, *IDH* wildtype glioblastoma, World Health Organization 2016 classification.

## Corresponding author:

Yeon-Lim Suh MD, PhD, Department of Pathology, Samsung Medical Center, Sungkyunkwan University School of Medicine, 81 Irwon-ro, Gangnam-gu, Seoul 135-710, South Korea (E-mail: [ylsuh76@skku.edu](mailto:ylsuh76@skku.edu))

Received 9 April 2019

Accepted 16 August 2019

Published Online Article

Accepted 21 August 2019

doi:10.1111/bpa.12782

## Abstract

The extremely invasive phenotypes and genotypes related to progression of gliomatosis cerebri (GC) remain unclear although GC has been removed as an independent entity from the 2016 WHO classification. Hence, categorization of GC under the current WHO molecular classification is essential, and the molecular subgroups that might contribute to GC progression should be compared with the histopathological differences between initial and new lesions identified during follow-up. Analyses of *IDH1/2* and *TERTp* mutations and 1p/19q co-deletion, and immunohistochemistry of *IDH1-R132H*, *ATRX*, p53 and galectin-3 were performed. Anaplastic astrocytoma, *IDH*-wildtype (AA-*IDHwt*) was the common molecular subgroup (52.8%), followed by diffuse astrocytoma, *IDH*-wildtype (DA-*IDHwt*) and AA, *IDH*-mutant (AA-*IDHmt*) (each 16.9%), DA-*IDHmt* (7.9%), glioblastoma (GBM)-*IDHwt* (3.3%) and GBM-*IDHmt* (2.2%). Approximately 92% of the AA-*IDHwt* lesions progressed to histologically confirmed GBM in the newly enhanced lesions harboring the *TERTp* mutation and expressing galectin-3. Similar to primary GBMs, GC-related GBMs that progressed from the *IDHwt* subgroups showed microvascular proliferation, palisading necrosis or thrombotic occlusion, implying that a subset of *IDHwt* subgroups may evolve to overt GBM. Molecular subgrouping did not provide the perfect prediction for the survival of GC patients. The AA-*IDHwt* group showed worse overall and progression-free survival (PFS) than the AA-*IDHmt* group. Biopsy plus radiotherapy, chemotherapy and temozolomide treatment for DA-*IDHwt*, and resection plus radiotherapy and temozolomide treatment for AA-*IDHwt* prolonged PFS. In conclusions, majority of GC was of the AA-*IDHwt* subgroup, which progressed to GBM. Molecular subgroups may assist in the selection of treatment modalities, because “GC pattern” still remains as a special growth of gliomas in WHO 2016 classification without established treatment guideline.

## INTRODUCTION

Although gliomatosis cerebri (GC), a rare and extensively infiltrating glioma involving multiple contiguous lobes of the brain, has been removed as an independent tumor entity from the 2016 WHO classification, it still remains a special “GC growth pattern” that can occur in both astrocytic and oligodendroglial tumors (2, 9, 24). Till date, both the phenotype and genotype of GCs remain unexplained (31). As described previously, the clinical behavior of GC is similar to that of WHO grade III gliomas, and secondary progression to highly malignant tumor may occur (5). However, the unique extremely invasive phenotype of GC is unlike

those of other ordinary high-grade gliomas (14), as GC infiltrates the brain extensively, but usually preserves the local parenchymal architecture, which is completely different from the destructive and necrotic infiltrating pattern observed in high-grade gliomas (5, 36). The significant neovascularization and mitotic activity that are commonly present in high-grade gliomas are not prominent features of GC (14, 31). Rather, the majority of GC tends to present histologically low-grade features such as rod cell-like astrocytic tumor cells with elongated fusiform nuclei without prominent microvascular proliferation or necrosis (5, 29). Because of the discrepancy between tumor behavior and histological grades

of GC, patients with GC show worse prognosis than patients with diffuse glioma of corresponding grades (5, 36).

Newly developed contrast-enhanced lesions on follow-up radiological images indicate the progression of GC (21). Although GC is first diagnosed using radiographic findings, which are subsequently supported by histopathological evaluation, the histological spectra of initial to newly developed lesions have been rarely specified. Therefore, histopathological review of new contrast-enhancing lesions and the initial lesions categorized under the current WHO 2016 molecular classification via consideration of *IDH* mutation as well as 1p/19q copy number status is required, which will improve our understanding regarding the relationship of genotype with GC progression.

The aim of this study was to classify GC into one of the WHO 2016 diagnostic categories of infiltrating glioma and analyze whether the molecular subgroups provide specific information regarding the histological and prognostic features of GC. We also attempted to determine the molecular subgroups that might contribute to the progression of GC and compared them with the histopathological observations on initial and newly developed lesions. This demonstrates the high-risk molecular subgroup within GCs for disease progression and clinical relevance of molecular subgrouping for selection of the best treatment in the clinic.

## PATIENTS AND METHODS

### Patients, histological and radiological evaluations and molecular classification

We retrospectively identified 100 consecutive patients with GC who were documented in the electronic database of the Samsung Medical Center during the 20-year period from 1995 to 2015 and whose informed consent was obtained from the patients. The diagnosis of GC was based on the following criteria (5, 29): (i) T2- or fluid-attenuated inversion recovery (FLAIR)-weighted magnetic resonance imaging (MRI) showing a diffuse process of infiltration involving more than three different lobes and relative preservation of the anatomical architecture and (ii) histological tissue analysis confirming glial cell proliferation, either diagnostic of or consistent with an infiltrative glioma. Eleven patients were excluded because of insufficient formalin-fixed paraffin-embedded (FFPE) tumor tissue from three patients and reclassification of six patients into glioblastoma (GBM), one patient into oligodendroglioma and one patient into “diffuse midline glioma,” among which four patients mainly affected in the thalamus or basal ganglia based on immunohistochemistry for H3.3-K27M. Finally, 89 patients, the features of whom were radiologically and histopathologically consistent with those of GC, were enrolled in this study. Among these 89 patients, 31 patients underwent second biopsy or surgical resection for histological examination of the newly developed contrast-enhancing lesions, which was absent in the previous studies involving follow-up brain imaging. The medical records and results of radiological investigations were reviewed to obtain clinical data. This study was approved

by the Institutional Review Board of the Samsung Medical Center (Seoul, Korea).

Neuropathologists (YLS and MJK) reviewed all the glass slides, and histological grading was based on a set of pathological factors (cellularity, nuclear atypia, mitoses, microvascular proliferation and necrosis) and was assigned to grades as follows: grade II, gliomas with mildly increased cellularity and mild nuclear atypia; grade III, gliomas with moderate hypercellularity with nuclear atypia or mildly increased cellularity with focal or dispersed anaplasia and mitotic activity (in biopsy samples); grade IV, high-grade glioma with severe hypercellularity, significant nuclear atypia and mitotic activity, microvascular proliferation and/or necrosis (5). Rod cells with fusiform hyperchromatic naked nuclei were considered present when the longer diameter was more than thrice that of the shorter diameter (29).

All MRIs were reviewed by a neuroradiologist and were classified as type 1 or type 2 GCs, according to a previously reported criterion (5, 29). Type 1 GCs were diffuse neoplastic growths and enlargements of the involved existing structure, without the formation of a discrete tumor mass at the initial clinical presentation (12). Type 2 GCs were lesions with an obvious neoplastic mass, in addition to a diffuse infiltrative lesion involving more than three different lobes at the time of diagnosis.

The molecular classification was based on the WHO 2016 classification of brain tumors as follows (24): (i) oligodendroglioma, *IDH* mutant and 1p/19q co-deleted; (ii) diffuse astrocytoma, *IDH* mutant (DA-*IDH*mt) or *IDH* wildtype (DA-*IDH*wt); (iii) anaplastic astrocytoma, *IDH* mutant (AA-*IDH*mt) or *IDH* wildtype (AA-*IDH*wt); (iv) glioblastoma, *IDH* mutant (GBM-*IDH*mt) or *IDH* wildtype (GBM-*IDH*wt).

### Mutational analysis of *IDH1*, *IDH2* and *TERT* promoters

Genomic DNA was extracted from 10 µm-thick sections of 10% neutral FFPE blocks using the Maxwell<sup>®</sup> 16 FFPE tissue LEV DNA purification kit (Promega, USA). *IDH1* (R132) and *IDH2* (R140 and R172) mutations were identified using PNAclap<sup>™</sup> *IDH1/2* mutation detection kit (PANAGENE, Daejeon, Korea) and *TERT* promoter (*TERTp*) mutations (C250 and C228) were identified using the PNAclap<sup>™</sup> *TERT* mutation detection kit (PANAGENE) according to the manufacturer's instructions. For equivocal cases, direct sequencing analyses of *IDH1*, *IDH2* and *TERTp* were repeated, as described previously (22).

### 1p/19q Co-deletion

While 25 cases were previously analyzed for 1p/19q status using fluorescence *in situ* hybridization (FISH) at the time of diagnosis, the remaining 64 cases were analyzed using PCR-based loss of heterozygosity test for the 1p/19q deletion (17, 18). Five microsatellite markers (D1S508, D1S2734, D1S186, D19S412 and D19S219) were used. For equivocal cases, FISH was performed on the FFPE tissue sections using probes for 1p36 and 19q13 (Vysis, Downers Grove,

IL, USA) (34). At least 100 non-overlapping neoplastic nuclei containing a minimum of two control signals were evaluated. No target signal or only a single signal was interpreted as a deletion. 1p deletion was defined by a combined target-to-control signal ratio  $<0.75$  or nucleus cutoff with 1 or 0 target signal  $>50\%$  (34). 19q deletion was defined by a combined target-to-control signal ratio  $<0.8$  and nucleus cutoff with 1 or 0 target signal  $>30\%$  (34).

### Immunohistochemistry

Immunohistochemical staining was performed on 4  $\mu\text{m}$ -thick FFPE sections using a Leica Microsystems Bond-Max autostainer system (Leica Biosystems, Wetzlar, Germany), according to the manufacturer's protocols (7, 19, 34). The primary antibodies included IDH1-R132H (clone H09, 1:10, Dianova, Hamburg, Germany), ATRX (HPA001906, 1:200, Sigma-Aldrich, St Louis, MO, USA), galectin-3 (9C4, 1:100, Novocastra, Newcastle, UK) and p53 (BP53-12, 1:400, Invitrogen, USA). IDH1-R132H expression was assessed by the presence of strong cytoplasmic staining in tumor cells (3, 22). Loss of nuclear staining in the majority of the tumor cells in the presence of an internal positive control (endothelium) was interpreted as loss of ATRX expression (34). Only nuclear staining of  $>5\%$  tumor cells was considered positive for p53, which has been previously validated as the appropriate cutoff value in our institute (7, 29). Galectin-3 was considered positive in the presence of both nuclear and cytoplasmic expression of tumor cells (23, 27).

### Statistical analysis

The Chi square test, Fisher's exact test and an independent t-test were used appropriately. Progression-free survival (PFS) was defined as the time between the first surgical intervention and the appearance of a new lesion on the follow-up MRI, as indicated by the treating clinician. Overall survival (OS) was defined as the period from the day of first surgery until death, or the end of follow-up. Analysis of the survival data was performed in September 2017. Survival differences among groups were calculated using the Kaplan-Meier method with a log-rank test. For the subgroup survival analysis, the log-rank test with Bonferroni's correction was used. All tests were two-tailed, and the significance level was set at 0.05. The SPSS statistical software (version 22, Statistical Package for the Social Sciences) was used for all statistical analyses.

## RESULTS

### Clinicopathological characteristics and patient management

Among the 89 patients, 52 (58.4%) were men and 37 (41.6%) were women, with median age of 49 years (range, 10–80 years) at the time of diagnosis. Based on the MRI findings, 65 tumors (73.0%) were classified as type 1 GC and 24 tumors (27.0%) as type 2 GC. In histological evaluation, histological

grade III (69.7%, 62/89) was the most common, followed by grade II (24.7%, 22/89) and grade IV (5.6%, 5/89). Hyperchromatic rod cells were variably observed in all the cases. The cellularity was predominantly mild (62.9%, 56/89) [22 into grade II, 33 into grade III and 1 into grade IV], followed by moderate (36.0%, 32/89) [29 into grade III and 3 into grade IV] and severe (1.1%, 1/89) [1 into grade IV]. Pleomorphic or multinucleated giant tumor cells were identified in 21 GCs (23.6%) [20 in grade III and 1 in grade IV]. Microvascular proliferation was detected in five GCs, which were classified as grade IV. Necrosis was not identified in 89 GCs. The representative histological observations of GC are shown in Figure 1.

Twenty-four patients (27.0%) underwent partial tumor resection and 65 patients (73.0%) underwent stereotactic biopsy for the purpose of histological diagnosis and decompression after the initial radiological diagnosis. Twenty-five patients underwent either partial tumor resection or biopsy and did not receive any further adjuvant treatment. Postoperative therapy usually included radiotherapy, with or without chemotherapy. In 65 resected patients, 6 patients (6.7%) received local radiotherapy, with conventional fractionation (2 Gy/fraction) and 58 Gy median total dose (range, 54–60 Gy). The extent of the radiotherapy was determined by the area of tumor involvement. Fourteen patients (15.7%) received adjuvant chemotreatment following radiotherapy, using temozolomide (TMZ) (6.7%) or nitrosourea-based regimen (2.3%) such as BCNU (carmustine-[1,3-bis (2-chloroethyl)-1-nitrosourea]) and PCV (procarbazine, carmustine and vincristine), and combined TMZ and nitrosourea-based chemotherapy (6.7%).

In 65 biopsied patients (73.0%), 14 patients (15.7%) received only radiotherapy. Twenty-three patients (25.9%) received adjuvant chemotherapy following radiotherapy, using TMZ (7.9%) or nitrosourea-based regimen (10.1%) and combined TMZ and nitrosourea-based chemotherapy (7.9%).

The follow-up period ranged from 2 to 128 months (mean  $\pm$  SD,  $31.1 \pm 27.5$  months). During the follow-up period, 69 patients (77.5%) died and 52 patients (58.4%) showed disease progression. The median survival time of patients with GC was 23 months. The percentages of 1-year OS, 2-year OS and 3-year OS for patients with GC were 78.7%, 43.8% and 25.8%, respectively.

### Molecular and immunohistochemical results and their associations with growth types

The summary of patient characteristics, molecular and immunohistochemical results and correlation coefficients with GC growth types are listed in Table S1.

The *IDH1* and *IDH2* mutations were successfully analyzed in all 89 samples; however, the analysis of the *TERTp* mutation was successful in 34 samples. *IDH1* mutations were detected in 24 (27.0%) out of 89 samples [23 in CGT > CAT (R132H) and 1 in CGT > AGT (R132S)]. No *IDH2* mutation (0%) was detected. The 1p/19q co-deletions were detected in three cases (3.4%), all of which were histological grade III astrocytic tumors with type 1

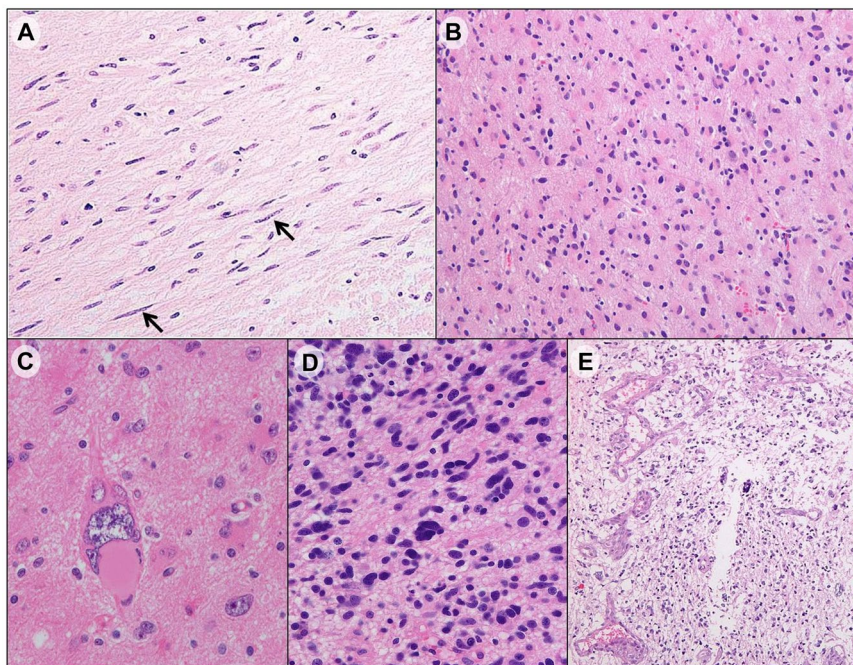


**Figure 1.** Representative histologic findings of gliomatosis cerebri. A. Infiltrating rod cells (Arrows) in anaplastic astrocytoma, *IDH* wildtype. B. Mildly increased cellularity and mild nuclear atypia in histological grade II (diffuse astrocytoma, *IDH* wildtype). C. Pleomorphic tumor cells

in anaplastic astrocytoma, *IDH* wildtype. D. Moderate hypercellularity with nuclear atypia in histological grade III (anaplastic astrocytoma, *IDH* mutant). E. Microvascular proliferation in glioblastoma, *IDH* wildtype.

GC. Two of them harboring 1p/19q co-deletions later progressed to GBMs. *TERTp* mutations were detected in 7 (20.6%) of 34 samples [three in C228T and four in C250T], all of which were type 1 GC of grade III ( $n = 6$ ) and grade IV ( $n = 1$ ) and showed intact *ATRX* expression. Hence, 1p/19q co-deletions and *TERTp* mutations were detected exclusively in Type 1 GCs.

The loss of *ATRX* expression was observed in 14 of 73 cases (19.2%), in which 11 were of type 1 GC and 3 were type 2 GC. p53 positivity was observed in 12 of 27 tumors (44.4%), all of which were type 1 GCs. p53 expression correlated with loss of *ATRX* expression (Spearman's correlation  $r = 0.441$ ;  $P = 0.035$ ). Galectin-3 was expressed in 6 of 20 tumors (30.0%), all of which were type 1 GCs and 50% (3/6) of the galectin-3 positive GCs later progressed to higher grades.

Regarding histological features, compared to type 2 GC, type 1 GC was significantly associated with lack of pleomorphic cells ( $P = 0.015$ ). The AA-IDHwt subgroup was the most common molecular subtype in both type 1 GC and type 2 GC, which accounted for 52.3% and 54.2% cases, respectively. There was no significant correlation between GC growth types and WHO 2016 molecular subgroups ( $P = 0.302$ ).

Overall, compared to type 2 GCs, the type 1 GCs appeared to show a trend toward high frequencies of 1p/19q co-deletions, loss of *ATRX* expression, *TERTp* mutations, p53 and galectin-3 expression and the AA-IDHwt subgroup, whereas they lacked pleomorphic tumor cells, although most of these associations did not reach statistical significance.

### Molecular Subgroupings and their correlation with survival

Based on the molecular subgroups of WHO 2016 classification (Table 1), all 89 GCs were classified into astrocytic tumors of 65 IDHwt (73.0%) [grade II (16.9%, 15/89), grade III (52.8%, 47/89) and grade IV (3.3%, 3/89)] and 24 IDHmt (27.0%) [grade II (7.9%, 7/89), grade III (16.9%, 15/89) and grade IV (2.2%, 2/89)]. No oligodendroglioma was designated to the 89 GCs, as three tumors harboring 1p/19q co-deletions did not fit the 2016 WHO criteria (*IDH* mutant and complete 1p/19q co-deleted) of oligodendrogliomas (two tumors showed AA-IDHwt and one showed a typical histology of GBM-IDHmt). These three cases with 1p/19q co-deletions were interpreted to harbor partial deletions involving the 1p36 and 19q13 by FISH, and their morphologies were astrocytic, without typical histological features of oligodendroglioma.

As a result, AA-IDHwt was the most common molecular subgroup in GC. AA-IDHwt harbored the most common *TERTp* mutation (4/7) and pleomorphic or multinucleated tumor giant cells (81.0%, 17/21), which was statistically higher than the number of pleomorphic cells of AA-IDHmt (14.3%, 3/21) ( $P = 0.038$ ).

Overall, molecular subgrouping did not provide statistically significant differences in OS and PFS in patients with GC ( $P = 0.078$  and  $P = 0.435$ , respectively; Figure 2A-B). The shortest median survival was 15 months for the GBM-IDHwt group, followed by 18 months for the AA-IDHwt, 24 months for the DA-IDHmt, 25 months for the DA-IDHwt, 43 months for the GBM-IDHmt and 58 months for the

**Table 1.** Clinicopathological characteristics according to WHO 2016 molecular subgrouping of gliomatosis cerebri. Bold indicates statistically significant ( $P < 0.05$ ). Abbreviations: IDHwt = IDH-wildtype; IDHmt = IDH-mutant; OS = overall survival.

	Total N = 89 (%)	IDHwt subgroups			IDHmt subgroups			P
		II n = 15 (16.9%)	III n = 47 (52.8%)	IV n = 3 (3.3%)	II n = 7 (7.9%)	III n = 15 (16.9%)	IV n = 2 (2.2%)	
Sex								0.927
Male	52 (57.4)	9 (60.0)	27 (57.4)	1 (33.3)	5 (71.4)	9 (60.0)	1 (50.0)	
Female	37 (41.6)	6 (40.0)	20 (42.6)	2 (66.7)	2 (28.6)	6 (40.0)	1 (50.0)	
Age (year)								0.794
<18	5 (5.6)	1 (6.7)	4 (8.5)	0 (0.0)	0 (0.0)	0 (0.0)	0 (0.0)	
≥18	84 (94.4)	14 (93.3)	43 (91.5)	3 (100)	7 (100)	15 (100)	2 (100)	
OS <sup>†</sup> time (month)	23	25	18	15	24	58	43	0.078
1 year-OS rate	78.7%	73.3%	72.3%	100%	85.7%	93.3%	100%	0.433
2 year-OS rate	43.8%	53.3%	31.9%	33.3%	42.9%	66.7%	100%	0.104
3 year-OS rate	25.8%	20.0%	17.0%	33.3%	28.6%	46.7%	100%	<b>0.044</b>
1p/19q								0.060
Co-deletion	3 (3.4)	0 (0.0)	2 (4.3)	0 (0.0)	0 (0.0)	0 (0.0)	1 (50.0)	
No codeletion	86 (96.6)	15 (100)	45 (95.7)	3 (100)	7 (100)	15 (100)	1 (50.0)	
ATRX (n = 73)								<0.001
Intact	59 (80.8)	13 (92.9)	38 (95.0)	1 (100)	2 (40.0)	5 (41.7)	0 (0.0)	
Loss	14 (19.2)	1 (7.1)	2 (5.0)	0 (0.0)	3 (60.0)	7 (58.3)	1 (100)	
TERTp (n = 34)								0.626
Wildtype	27 (79.4)	5 (100)	11 (73.3)	1 (100)	2 (100)	7 (77.8)	1 (50.0)	
Mutated	7 (20.6)	0 (0.0)	4 (26.7)	0 (0.0)	0 (0.0)	2 (22.2)	1 (50.0)	
P53 (n = 27)								0.103
Positive	12 (44.4)	1 (20.0)	4 (28.6)	1 (100)	2 (100)	3 (75.0)	1 (100)	
Negative	15 (55.6)	4 (80.0)	10 (71.4)	0 (0.0)	0 (0.0)	1 (25.0)	0 (0.0)	
Galectin-3 (n = 20)								0.230
Positive	6 (30.0)	1 (20.0)	5 (55.6)	-	0 (0.0)	0 (0.0)	0 (0.0)	
Negative	14 (70.0)	4 (80.0)	4 (44.4)	-	2 (100)	3 (100)	1 (100)	
Pleomorphic cells								<b>0.038</b>
Absent	68 (76.4)	15 (100)	30 (63.8)	2 (66.7)	7 (100)	12 (80.0)	2 n	
Present	21 (23.6)	0 (0.0)	17 (36.2)	1 (33.3)	0 (0.0)	3 (20.0)	0 (0.0)	

<sup>†</sup>OS time indicates median survival time.

AA-IDHmt groups, which showed a trend toward shorter survival along with increase in histological grades in the IDHwt subgroups.

Comparison between subgroups revealed that the AA-IDHwt ( $31.5 \pm 5.3$  months) and GBM-IDHwt groups ( $23.7 \pm 8.7$  months) showed statistically worse OS than the AA-IDHmt subgroup ( $54.5 \pm 9.7$  months) ( $P = 0.007$  and  $P = 0.032$ , respectively). The AA-IDHwt subgroup ( $27.4 \pm 5.4$  months) also showed statistically poorer PFS than the AA-IDHmt subgroup ( $41.7 \pm 8.7$  months) ( $P = 0.034$ ). There were no statistically significant prognostic differences between the other molecular subgroups.

### Survival and prognosis

We also evaluated the prognostic impact of the histological grades, GC growth types and *IDH* or *TERTp* mutational status on survival of patients with GC. The presence of *IDH1* mutation (median 55 months) was associated with better OS than that of wild-type *IDH1* (median 18 months) in all patients ( $P = 0.006$ ), whereas the *IDH1* mutation showed a trend of borderline association with favorable PFS ( $P = 0.066$ ) (Figure 2C,D). However, OS or PFS did not

vary significantly among GCs with respect to GC growth types, *TERTp* mutational status, or histological grades ( $P = 0.625$  and  $P = 0.321$ ;  $P = 0.455$  and  $P = 0.098$ ;  $P = 0.805$  and  $P = 0.858$ , respectively).

In multivariate analysis (Table 2), the presence of *IDH1* mutation was the only independent favorable prognostic factor predicting increased OS [ $P = 0.009$ , HR 0.201, 95% CI 0.060–0.671]. In addition, the *IDH1* mutation, partial resection, *TERTp* wildtype and absence of newly developed enhancing lesion were independent favorable prognostic factors associated with increased PFS in patients [ $P = 0.010$ , HR 0.247, 95% CI 0.086–0.712;  $P = 0.021$ , HR 0.204, 95% CI 0.053–0.785;  $P = 0.009$ , HR 5.334, 95% CI 1.519–18.729;  $P = 0.004$ , HR 6.099, 95% CI, 1.754–21.204, respectively].

Prognostic correlations depending on the treatment modalities including biopsy (Bx) or partial tumor resection (Rx) with or without radiotherapy (RT), nitrosourea-based chemotherapy (CTx) and TMZ were further investigated. The most favorable median OS periods were observed in Rx + RT + TMZ (91 months), followed by Bx + TMZ (37 months), Bx + RT + CTx + TMZ (31 months), Bx + RT + CTx (25 months), Bx only (21 months), Bx + RT + TMZ (17 months), Rx + RT + CTx (15 months)

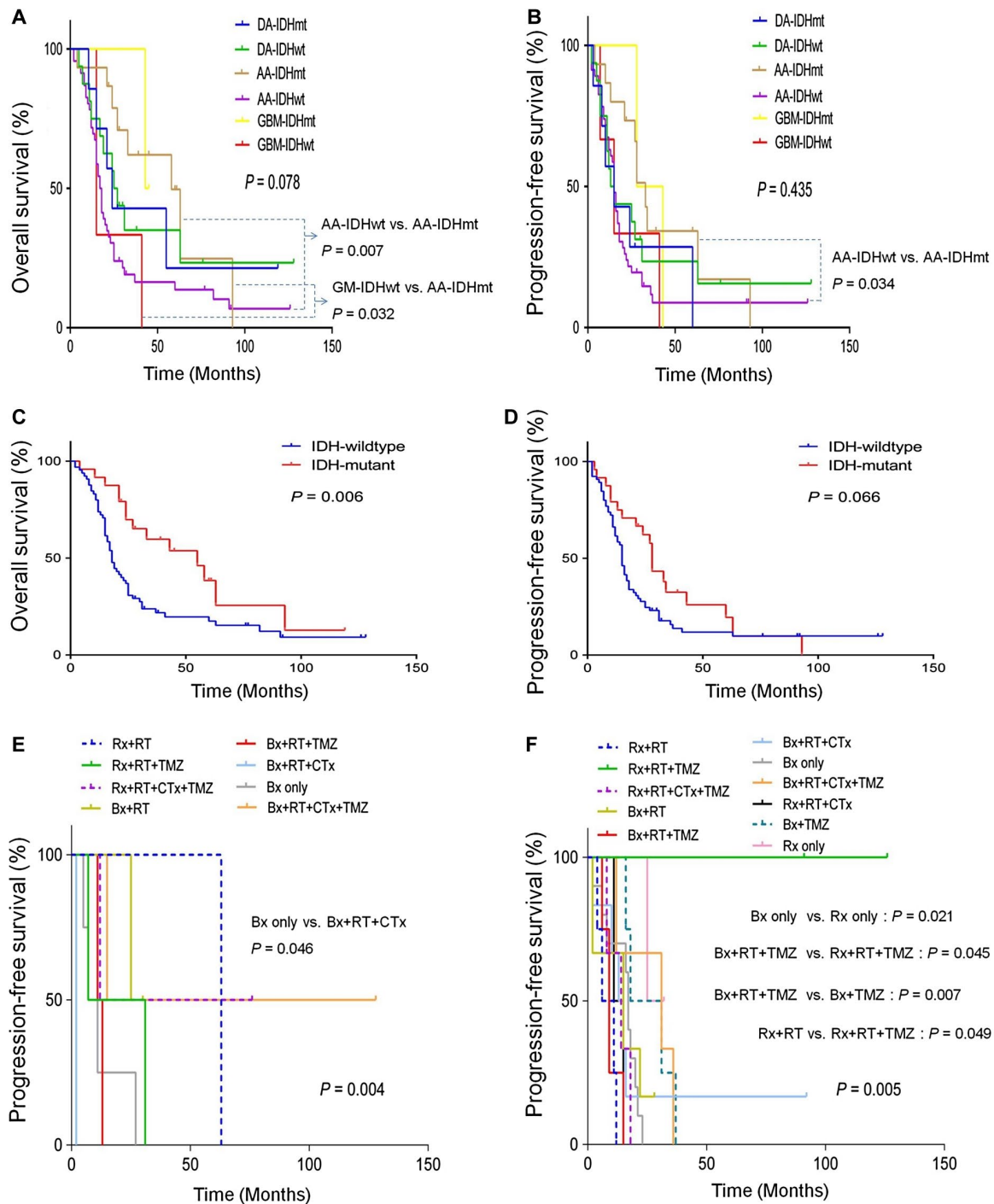


**Figure 2.** Overall survival (OS) (A) and progression-free survival (PFS) (B) in gliomatosis cerebri (GC) according to WHO 2016 molecular subgroups. OS (C) and PFS (D) according to *IDH* mutational status. PFS according to treatment modalities in DA-IDHwt subgroup (E) and AA-IDHwt subgroup (F).

and Bx + RT (15 months), Rx + RT + CTx + TMZ (14 months) and Rx + RT (12 months). The most favorable median PFS was detected in Rx only (34 months), followed by Bx + TMZ (31 months), Bx + RT + CTx + TMZ (27 months), Bx only (18 months), Bx + RT + CTx

(15 months) and Bx + RT (15 months), Rx + RT + CTx + TMZ (13 months), Rx + RT (11 months), Rx + RT + CTx (11 months) and Bx + RT + TMZ (11 months).

Among the WHO 2016 molecular subgroups, the DA-IDHwt and AA-IDHwt subgroups showed statistically

**Table 2.** Multivariate analyses for overall survival and progression-free survival using the Cox proportional hazard model. Abbreviations: HR = hazard ratio; CI = confidential interval; TMZ = temozolomide.

	Overall survival		Progression-free survival	
	HR (95% CI)	<i>P</i>	HR (95% CI)	<i>P</i>
Age (year) (>18 vs. ≤18)	0.232 (0.023–2.352)	0.216	0.697 (0.091–5.305)	0.727
Sex (male vs. female)	1.518 (0.441–5.232)	0.508	1.171 (0.375–3.662)	0.786
<i>IDH1</i> (Wildtype vs. Mutated)	0.201 (0.060–0.671)	0.009	0.247 (0.086–0.712)	0.021
<i>TERTp</i> (Wildtype vs. Mutated)	2.581 (0.650–10.255)	0.178	5.334 (1.519–18.729)	0.009
Growth type (type 1 vs. type 2)	0.206 (0.024–1.765)	0.149	0.983 (0.187–5.170)	0.984
Histological grade (II-III vs. IV)	1.591 (0.411–6.160)	0.501	0.763 (0.215–2.705)	0.676
Newly enhancing lesion (yes vs. no)	1.483 (0.462–4.757)	0.507	6.099 (1.754–21.204)	0.004
Partial resection (yes vs. no)	0.294 (0.071–1.226)	0.093	0.204 (0.053–0.785)	0.021
Radiotherapy (yes vs. no)	0.736 (0.204–2.660)	0.641	0.757 (0.228–2.513)	0.649
Chemotherapy <sup>†</sup> (yes vs. no)	2.039 (0.484–8.581)	0.331	2.590 (0.632–10.616)	0.186
TMZ (yes vs. no)	2.787 (0.767–10.128)	0.119	2.774 (0.825–9.327)	0.099

<sup>†</sup>Nitrosourea-based chemotherapy.

significant differences in PFS depending on treatment modalities ( $P = 0.004$  and  $P = 0.005$ , respectively) (Figure 2E-F). However, no other molecular subgroup showed statistically significant differences in OS or PFS with respect to treatments.

In the DA-IDHwt subgroup, Bx + RT + CTx + TMZ (median 71.5 months) showed the best outcomes, followed by Rx + RT (63 months), Bx + RT (27.5 months), Rx + RT + TMZ (19 months), Rx + RT + CTx + TMZ (12 months), Bx + RT + TMZ (12 months), Bx only (9 months) and Bx + RT + CTx (2 months). As a result, Bx + RT + CTx + TMZ led to the most favorable PFS, whereas Bx + RT + CTx resulted in a PFS worse than those observed with other treatment modalities in the DA-IDHwt subgroups.

In the AA-IDHwt subgroup, Rx + RT + TMZ (108.5 months) showed the best outcomes of PFS, followed by Bx + RT + CTx + TMZ (31 months), Rx only (28.5 months), Bx + TMZ (24.5 months), Bx only (17 months), Rx + RT + CTx + TMZ (16 months), Bx + RT (15 months), Bx + RT + CTx (14 months), Rx + RT + CTx (13 months), Bx + RT + TMZ (9 months) and Rx + RT (median 8.5 months). As a result, Rx + RT + TMZ showed the most favorable PFS, whereas Rx + RT tended to show the worst PFS compared to other treatments in the AA-IDHwt subgroups. Taken together, Bx + RT + CTx + TMZ for the DA-IDHwt subgroup and Rx + RT + TMZ for the AA-IDHwt subgroup increased PFS rates in GCs.

In particular, several therapeutic options were statistically better for PFS of the AA-IDHwt subgroup; for example, Rx only was better than Bx only ( $P = 0.021$ ), Rx + RT + TMZ was better than Bx + RT + TMZ ( $P = 0.045$ ), Bx + TMZ was better than Bx + RT + TMZ ( $P = 0.007$ ) and Rx + RT + TMZ was better than Rx + RT ( $P = 0.049$ ).

For 12 patients, there was an unusually long OS of >5 years after diagnosis of GC (range 61–128 months) (Table 3). Prominent therapeutic modalities were not identified in these patients. However, the effects of Bx + RT + CTx + TMZ for the DA-IDHwt subgroup and Rx + RT + TMZ

for the AA-IDHwt subgroup were also well appreciated in two patients who survived >10 years. These patients were female with type 2 GC of the IDHwt subgroups (DA-IDHwt and AA-IDHwt) who underwent treatment, including radiotherapy and TMZ.

### Histopathological comparison between initial lesion at first diagnosis and newly developed contrast-enhancing lesion during follow-up

The median interval time to new appearance of contrast-enhancing lesions in follow-up MRI was 13 months, ranging from 1 to 89 months. Thirty-one patients were available for histological review of both initial and later newly-developed lesions. However, two cases were excluded because of complete necrosis in the follow-up biopsied specimens, and the remaining 29 specimens were only evaluated for histological comparisons (Table S2). The schematic diagnostic spectra from initial lesion to disease progressed lesion have been summarized in Figure 3.

The newly developed contrast-enhancing lesions initially originated from 20 IDHwt subgroups (69.0%) [7 grade II (24.2%), 12 grade III (41.4%), and 1 grade IV (3.4%)] and 9 IDHmt subgroups (31.0%) [5 grade II (17.2%) and 4 grade III (13.8%)]. Of those 29 cases, 20 (69.0%) [16 IDHwt (55.2%) and 4 IDHmt (13.8%)] progressed to grades higher than the initial grades, in which 15 cases (51.7%), including 13 IDHwt (44.8%) [2 DA-IDHwt and 11 AA-IDHwt] and 2 DA-IDHmt (6.9%), developed to GBM. The remaining five grade II cases [three DA-IDHwt (60.0%) and two DA-IDHmt (40.0%)] cases became grade III lesions. The median interval times to GBM progression were 13 months for the IDHwt subgroups (range 1–34 months) and 7.5 months for the IDHmt subgroups (range 2–13 months). However, none of the AA-IDHmt subgroups progressed to GBM. In contrast, the histological grades of the remaining nine cases of contrast-enhancing new lesions (31.0%), including four IDHwt [two grade II, one grade III, one grade IV] and five IDHmt [one grade II and four grade III], were identical to the initial grades.

**Table 3.** Clinicopathological characteristics from shorter survival to longer survival time of 12 patients who lived more than 5 years after diagnosis of gliomatosis cerebri. Abbreviations: OS = overall survival; DA-IDHwt = Diffuse astrocytoma, IDH-wildtype; DA-IDHmt = Diffuse astrocytoma, IDH-mutant; AA-IDHwt = Anaplastic astrocytoma, IDH-wildtype; AA-IDHmt = Anaplastic astrocytoma, IDH-mutant; F = female; M = male; Rx = resection; RT = radiotherapy; TMZ = temozolomide; Bx = biopsy; CTx = nitrosourea-based chemotherapy.

No.	WHO2016	OS (month)	Survival	Sex	Age (year)	Growth type	Treatment†
1	AA-IDHmt	61	Alive	M	42	Type 2	Rx
2	AA-IDHmt	63	Died	M	28	Type 2	Bx RT
3	DA-IDHwt	63	Died	M	52	Type 1	Rx RT
4	DA-IDHwt	76	Alive	F	48	Type 2	Rx RT CTx TMZ
5	AA-IDHwt	77	Alive	M	40	Type 1	Bx TMZ
6	AA-IDHwt	82	Died	F	49	Type 1	Bx RT CTx TMZ
7	AA-IDHwt	91	Died	M	55	Type 2	Rx RT TMZ
8	AA-IDHwt	92	Alive	M	15	Type 1	Bx RT CTx
9	AA-IDHmt	93	Died	F	28	Type 2	Rx RT TMZ
10	DA-IDHmt	119	Alive	M	68	Type 1	Bx RT TMZ
11	AA-IDHwt	126	Alive	F	49	Type 2	Rx RT GKs TMZ
12	DA-IDHwt	128	Alive	F	51	Type 2	Bx Bx RT CTx TMZ

†Treatment includes the overall treatment after initial biopsy or resection before follow-up biopsy.

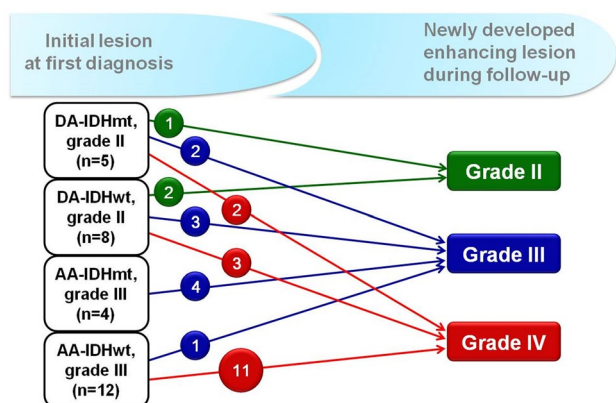


**Figure 3.** Diagnostic spectrums from initial lesion to newly developed contrast-enhanced lesions during the follow-up.

## DISCUSSION

In the present study, we have shown that AA-IDHwt is the most common molecular subgroup (52.8%) in GC, with approximately 92% (11/12) of AA-IDHwt exhibiting progression to GBM in the newly enhanced lesions. Molecular subgrouping, according to the 2016 WHO classification, did not accurately predict the survival of patients with GC. However, the AA-IDHwt subgroup showed worse prognoses in terms of both OS and PFS than the AA-IDHmt subgroup. We also observed that Bx + RT + CTx + TMZ treatment for the DA-IDHwt subgroup and Rx + RT + TMZ treatment for the AA-IDHwt subgroup prolonged the PFS rates. To the best of our knowledge, this is the first study demonstrating the differences between the histological spectra of initial and progressed lesions, and the clinical outcomes of the treatment modalities depend on specific molecular subgroups in GC.

Fifty percent GCs was subcategorized into AA-IDHwt, followed by DA-IDHwt (16.9%), AA-IDHmt (16.9%), DA-IDHmt (7.9%), GBM-IDHwt (3.3%) and GBM-IDHmt

(2.2%). No oligodendroglioma was identified. The majority of GCs were IDHwt subgroups (73.0%), with the most common being AA-IDHwt. A prominent histological feature of the AA-IDHwt subgroup was the high frequency of occurrence (81.0%) of pleomorphic cells, which distinguished it from the AA-IDHmt subgroup. In the newly developed enhancing lesions observed during follow-up, AA-IDHwt and DA-IDHwt comprised the two top-ranking molecular subgroups progressing to GBM. Interestingly, the *TERTp* mutation was only identified in the AA-IDHwt subgroup, which later progressed to GBM. Galectin-3 expression was also positive in the DA-IDHwt and AA-IDHwt subgroups, which later progressed to GBM. The *TERTp* mutation is related to the transformation of glial progenitor cells to primary GBM and its associated aggressive phenotype (15, 24, 28). Galectin-3 expression in glial tumor cells has been reported to be related to infiltrative cell motility away from hypoxic regions (27). Our molecular and immunohistochemical observations are interesting in the context of previously published data, as GC has been considered a lesion of intermediate malignancy in the progression of diffuse glioma to GBMs, and the progression of GC is mediated by tumor stem cells (20). As GC shares characteristics with neural stem cells, GC may show migratory behavior, diversity of progeny and proliferative potential (20). Herrlinger *et al* (9) have shown that 52.2% GCs show GBM-IDHwt-associated methylation profile, suggesting a close relationship between GC and GBM at the molecular level. Recently, IDHwt *TERTp*-mutated astrocytomas were found to be typically present as GC in one series (11), suggesting that IDHwt GCs indeed possessed the potential of malignant transformation to GBMs. In fact, rapid transformations from initially *IDH1*-wildtype, low-grade GC without contrast-enhancement on MRI to massive GBM or higher-grade glioma have been rarely reported within the short interval of 3–7 months after initial presentation (13, 16, 26, 32, 35).



In addition, the newly appeared GBM originating from the IDHwt subgroups showed microvascular proliferation ( $n = 3$ ), palisading necrosis ( $n = 2$ ) or thrombotic occlusion ( $n = 1$ ), which are not related to therapeutic effects, but rather corresponded to typical histological features of primary GBM. These differences in the histological spectra between initial and progressed lesions may contradict the well-known mechanism that only IDHwt low-grade gliomas secondarily succumb to GBM, as well as the fact that GBM-IDHwt arise *de novo* with no precursor lesions (24). Nevertheless, we observed that a considerable number of IDHwt GCs truly progressed to GBM-IDHwt in our study, implying a subset of IDHwt subgroups may be precursors or early-stage GBMs that ultimately evolve to overt GBM.

Molecular subgrouping, according to the WHO 2016 classification, did not provide detailed prognostic stratification for patients with GC. Rather, the presence of the *IDH1* mutation in GC patients demonstrated independent favorable prognostic factor for both OS and PFS. The favorable prognostic value of *IDH1* mutations has been consistently reported in patients with GC (4, 6, 22). The absence of reliable prognostic and predictive markers for GCs despite application of the WHO 2016 molecular subgrouping guidelines, highlights the importance of *IDH1* mutation status in patients with GCs.

While palliative surgery, radiotherapy and chemotherapy have been used to treat patients with GCs, the optimal therapeutic strategy for GCs remains unclear. There is no standard guideline for surgery and the extent of surgical resection in GC. A previous study has reported that any survival benefit is not provided between partial resection and biopsy (median survival, 18 vs. 21 months) in 30 GC patients (30). Radiotherapy has been reported to be effective in approximately 50% patients with GCs and to increase OS (10). However, large field radiotherapy is associated with the risk of severe toxicity. Chemotherapy is often administered to patients with GC, and upfront chemotherapy produces an objective radiological response rate in 25%–45% patients and a median PFS of 13–17 months (6, 14). However, its efficacy still remains controversial. TMZ is currently widely used as a first-line treatment for GCs because it is more tolerable and less toxic than nitrosourea-based chemotherapy (14), and may be a cost-effective treatment for GC (33). In these circumstances, the molecular subgrouping within GC may be of considerable clinical significance for guided decision-making regarding the appropriate therapeutic strategy. Especially, we have shown that Bx + RT + CTx + TMZ therapy for the DA-IDHwt subgroup and Rx + RT + TMZ therapy for the AA-IDHwt subgroup increased PFS rates in GCs. In particular, in the AA-IDHwt subgroup, RT + TMZ may be recommended post-resection but not post-biopsy. After tumor resection, RT + TMZ may be related to more favorable PFS than RT. However, after biopsy, initial TMZ may be recommended instead of RT + TMZ. In the context, the effects of Bx + RT + CTx + TMZ for the DA-IDHwt subgroup and Rx + RT + TMZ for the AA-IDHwt subgroup were

also well appreciated in two patients who unusually survived >10 years. Although a long indolent course and prolonged survival are rarely observed in GC patients (8), the reasons for long survivors with GC should be further more clearly elucidated in the future study. Therefore, our study suggests that molecular subgrouping may allow prediction of clinical outcomes regarding treatments and enable selection of patients who might benefit from treatment.

In our GCs, four cases were located in the midline, in addition to more than three cerebral lobes, which were used for immunohistochemistry for H3.3-K27M. Among them, only one case of a 31-year-old male was confirmed via H3.3-K27M positivity as diffuse midline glioma and was excluded from the current study. The characteristics of adult H3-K27M mutant gliomas in association with GC are yet to be completely elucidated (25, 31). Whether GC with H3-K27M mutation may represent a rare molecular pattern of GCs or not requires further investigation.

Based on our results, it could not be conclusive that GC is a specific subtype of diffuse gliomas pathologically and prognostically. The current WHO 2016 classification describes “GC pattern” only in *IDH*-wildtype gliomas (24). However, the present study has shown that GC consists of both *IDH*-wildtype and *IDH*-mutant subtypes, although the majority of GCs are AA-IDHwt that would progress to GBM. The prognosis of GC is importantly related to *IDH* mutational status. The favorable prognosis would be anticipated when the therapeutic strategies such as concurrent chemoradiation indicative of GBM are applied to GC patients, regardless the histological grades.

The limitations of the current study are a lack of entire GC lesions caused by resection or biopsy samples for possible regional heterogeneity. Unfortunately, because of sample limitations we could not fully evaluate all cases for genetic alterations associated with *IDH*-wildtype astrocytic tumors that are proposed by the Consortium to Inform Molecular and Practical Approaches to CNS Tumor Taxonomy (cIMPACT-NOW) recently issued update 3 (1), because of insufficient sample quantity mostly obtained from stereotactic biopsy for additional molecular study. The current study also took long time until accomplishing both molecular and immunohistochemical results, their validations and repeated experiments for confirmation before recent cIMPACT-NOW recommendation. Nevertheless, we were able to interpret several trends from these results. AA-IDHwt was the most common molecular subgroup of GC and was also the most remarkable subgroup potentially progressing to GBM. Molecular subgrouping within GC appears to be insufficient to completely explain the survival outcomes of GC, highlighting the importance of *IDH1* mutation predicting favorable survival in GC. Because the term of “GC pattern” still remains as a special growth of gliomas in WHO 2016 classification with neither established prognostic and predictive markers nor treatment guideline in GC, molecular subgroups may indicate the best treatment options for GC patients, who might benefit from various treatment modalities.

## ACKNOWLEDGMENTS

This work was supported by the National Research Foundation of Korea (NRF) grant funded by the Korea government (Ministry of Science and ICT) (No. NRF-2019R1C1C1004463).

## AUTHOR CONTRIBUTIONS

Yeon-Lim Suh and Mi Jung Kwon designed the study, interpreted the data, wrote the manuscript and drafted of the manuscript; So Young Kang carried out the experiments and data acquisition; Haeyon Cho, Jung Il Lee and Sung Tae Kim were involved in the acquisition, analysis or interpretation of clinical data.

## CONFLICTS OF INTEREST

All authors have no conflicts of interests to disclose.

## DATA AVAILABILITY STATEMENT

Data available on request because of privacy/ethical restrictions. The data that support the findings of this study are available on request from the corresponding author.

## REFERENCES

1. Brat DJ, Aldape K, Colman H, Holland EC, Louis DN, Jenkins RB *et al* (2018) cIMPACT-NOW update 3: recommended diagnostic criteria for “Diffuse astrocytic glioma, IDH-wildtype, with molecular features of glioblastoma, WHO grade IV”. *Acta Neuropathol* **136**:805–810.
2. Broniscer A, Chamdine O, Hwang S, Lin T, Pounds S, Onar-Thomas A *et al* (2016) Gliomatosis cerebri in children shares molecular characteristics with other pediatric gliomas. *Acta Neuropathol* **131**:299–307.
3. Capper D, Weissert S, Balss J, Habel A, Meyer J, Jager D *et al* (2009) Characterization of R132H mutation-specific IDH1 antibody binding in brain tumors. *Brain Pathol* **20**:245–254.
4. Desestret V, Ciccarino P, Ducray F, Criniere E, Boisselier B, Labussiere M *et al* (2011) Prognostic stratification of gliomatosis cerebri by IDH1(R132H) and INA expression. *J Neurooncol* **105**:219–224.
5. Fuller GN, Kros JM (2007) Gliomatosis cerebri. In: WHO Classification of Tumours of the Central Nervous System, Louis DN, Ohgaki H, Wiestler OD, Cavenee WK, Ellison DW, Figarella-Branger D *et al* (eds), pp. 50–52. IARC Press: Lyon.
6. Glas M, Bahr O, Felsberg J, Rasch K, Wiewrodt D, Schabet M *et al* (2011) NOA-05 phase 2 trial of procarbazine and lomustine therapy in gliomatosis cerebri. *Ann Neurol* **70**:445–453.
7. Ha SY, Kang SY, Do IG, Suh YL (2013) Glioblastoma with oligodendroglial component represents a subgroup of glioblastoma with high prevalence of IDH1 mutation and association with younger age. *J Neurooncol* **112**:439–448.
8. Herrlinger U, Felsberg J, Kuker W, Bornemann A, Plasswilm L, Knobbe CB *et al* (2002) Gliomatosis cerebri: molecular pathology and clinical course. *Ann Neurol* **52**:390–399.
9. Herrlinger U, Jones DTW, Glas M, Hattungen E, Gramatzki D, Stuplich M *et al* (2016) Gliomatosis cerebri: no evidence for a separate brain tumor entity. *Acta Neuropathol* **131**:309–319.
10. Inoue T, Kumabe T, Kanamori M, Sonoda Y, Watanabe M, Tominaga T (2011) Prognostic factors for patients with gliomatosis cerebri: retrospective analysis of 17 consecutive cases. *Neurosurg Rev* **34**:197–208.
11. Izquierdo C, Barritault M, Poncet D, Cartalat S, Joubert B, Bruna J *et al* (2018) Radiological Characteristics and Natural History of Adult IDH-Wildtype Astrocytomas with TERT Promoter Mutations. *Neurosurgery* **85**:E448–E456.
12. Jennings MT, Frenchman M, Shehab T, Johnson MD, Creasy J, LaPorte K, Dettbarn WD (1995) Gliomatosis cerebri presenting as intractable epilepsy during early childhood. *J Child Neurol* **10**:37–45.
13. Jimenez Caballero PE, Mollejo Villanueva M, Marsal Alonso C (2007) Gliomatosis cerebri: evolution to glioblastoma multiforme. *Neurologia* **22**:395–398.
14. Kaloshi G, Everhard S, Laigle-Donadey F, Marie Y, Navarro S, Mokhtari K *et al* (2008) Genetic markers predictive of chemosensitivity and outcome in gliomatosis cerebri. *Neurology* **70**:590–595.
15. Killela PJ, Reitman ZJ, Jiao Y, Bettgowda C, Agrawal N, Diaz LA Jr *et al* (2013) TERT promoter mutations occur frequently in gliomas and a subset of tumors derived from cells with low rates of self-renewal. *Proc Natl Acad Sci USA* **110**:6021–6026.
16. Kim Y, Hong M, Do IG, Ha SY, Lee D, Suh YL (2015) Wnt5a, Ryk and Ror2 expression in glioblastoma subgroups. *Pathol Res Pract* **211**:963–972.
17. Kim SH, Kim H, Kim TS (2005) Adequate microsatellite markers for 1p/19q loss of heterozygosity of oligodendroglial tumors in Korean patients. *Korean J Pathol* **39**:22–33.
18. Kim SH, Kim H, Kim TS (2005) Clinical, histological, and immunohistochemical features predicting 1p/19q loss of heterozygosity in oligodendroglial tumors. *Acta Neuropathol* **110**:27–38.
19. Kim HK, Yu IK, Kim SM, Kim JH, Lee SH, Lee SY (2017) Rapid progression of gliomatosis cerebri to secondary glioblastoma, factors that affect the progression rate: a case report. *J Korean Soc Radiol* **76**:221–228.
20. Kong DS, Kim ST, Lee JI, Suh YL, Lim DH, Kim WS *et al* (2010) Impact of adjuvant chemotherapy for gliomatosis cerebri. *BMC Cancer* **10**:424.
21. Kong DS, Kim MH, Park WY, Suh YL, Lee JI, Park K *et al* (2008) The progression of gliomas is associated with cancer stem cell phenotype. *Oncol Rep* **19**:639–643.
22. Kwon MJ, Kim ST, Kwon MJ, Kong DS, Lee D, Park S *et al* (2012) Mutated IDH1 is a favorable prognostic factor for type 2 gliomatosis cerebri. *Brain Pathol* **22**:307–317.
23. Kwon MJ, Sung CO, Kang SY, Do IG, Suh YL (2013) Differential expression of extracellular matrix-related genes in rare variants of meningioma. *Hum Pathol* **44**:260–268.
24. Louis DN, von Deimling A, Cavenee WK (2016) Diffuse astrocytic and oligodendroglial tumours. In: WHO Classification of Tumours of the Central Nervous System, Louis DN, Ohgaki H, Wiestler OD, Cavenee WK, Ellison DW, Figarella-Branger D *et al* (eds), Chapter 1, pp. 15–77. IARC Press: Lyon.

25. Meyronet D, Esteban-Mader M, Bonnet C, Joly MO, Uro-Coste E, Amiel-Benouaich A *et al* (2017) Characteristics of H3 K27M-mutant gliomas in adults. *Neuro Oncol* **19**:1127–1134.
26. Nagata R, Ikeda K, Nakamura Y, Ishikawa Y, Miura K, Sato R *et al* (2010) A case of gliomatosis cerebri mimicking limbic encephalitis: malignant transformation to glioblastoma. *Intern Med* **49**:1307–1310.
27. Nader L, Marie SK, Carlotti CG Jr, Gabbai AA, Rosemberg S, Malheiros SM *et al* (2004) Galectin-3 as an immunohistochemical tool to distinguish pilocytic astrocytomas from diffuse astrocytomas, and glioblastomas from anaplastic oligodendrogliomas. *Brain Pathol* **14**:399–405.
28. Ohgaki H, Kleihues P (2013) The definition of primary and secondary glioblastoma. *Clin Cancer Res* **19**:764–772.
29. Park S, Suh YL, Nam DH, Kim ST (2009) Gliomatosis cerebri: clinicopathologic study of 33 cases and comparison of mass forming and diffuse types. *Clin Neuropathol* **28**:73–82.
30. Perkins GH, Schomer DF, Fuller GN, Allen PK, Maor MH (2003) Gliomatosis cerebri: improved outcome with radiotherapy. *Int J Radiat Oncol Biol Phys* **56**:1137–1146.
31. Ranjan S, Warren KE (2017) Gliomatosis cerebri: current understanding and controversies. *Front Oncol* **7**:165.
32. San Millan B, Kaci R, Polivka M, Robert G, Heran F, Gueguen A *et al* (2010) Gliomatosis cerebri: a biopsy and autopsy case report. *Ann Pathol* **30**:25–29.
33. Sanson M, Cartalat-Carel S, Taillibert S, Napolitano M, Djafari L, Cougnard J *et al* (2004) Initial chemotherapy in gliomatosis cerebri. *Neurology* **63**:270–275.
34. Sim J, Nam DH, Kim Y, Lee IH, Choi JW, Sa JK, Suh YL (2018) Comparison of 1p and 19q status of glioblastoma by whole exome sequencing, array-comparative genomic hybridization, and fluorescence in situ hybridization. *Med Oncol* **35**:60.
35. Sun P, Piao H, Guo X, Wang Z, Sui R, Zhang Y *et al* (2014) Gliomatosis cerebri mimicking acute viral encephalitis and with malignant transformation of partial lesions: a case report. *Exp Ther Med* **8**:925–928.
36. Vates GE, Chang S, Lamborn KR, Prados M, Berger MS (2003) Gliomatosis cerebri: a review of 22 cases. *Neurosurgery*. **53**:261–271; discussion 271.

## SUPPORTING INFORMATION

Additional supporting information may be found in the online version of this article at the publisher's web site:

**Table S1.** Patient characteristics of 89 patients with gliomatosis cerebri and correlations between growth type and clinicopathological characteristics.

**Table S2.** Clinicopathological features of the 29 patients with second biopsy at disease progression site during follow-up.